On Woven Fabric Sound Absorption Prediction

Iwan PRASETIYO[(1)], Gradi DESENDRA[(1)], Melissa N. HERMANTO[(1)], Damar R. ADHIKA[(1), (2)]

[(1)] *Engineering Physics*
Faculty of Industrial Technology
Institut Teknologi Bandung
Ganesa 10, Bandung 40132, Indonesia; e-mail: i.prasetiyo@fti.itb.ac.id

[(2)] *National Research Center for Nanotechnology*
Institut Teknologi Bandung
Ganesha 10, Bandung 40132, Indonesia

For building applications, woven fabrics have been widely used as finishing elements of room interior but not in particular aimed for sound absorbers. Considering the micro perforation of the woven fabrics, they should have potential to be used as micro-perforated panel (MPP) absorbers; some measurement results indicated such absorption ability. Hence, it is of importance to have a sound absorption model of the woven fabrics to enable us predicting their sound absorption characteristic that is beneficial in engineering design phase. Treating the woven fabric as a rigid frame, a fluid equivalent model is employed based on the formulation of Johnson-Champoux-Allard (JCA). The model obtained is then validated by measurement results where three kinds of commercially available woven fabrics are evaluated by considering their perforation properties. It is found that the model can reasonably predict their sound absorption coefficients. However, the presence of perturbations in pores give rise to inaccuracy of resistive component of the predicted surface impedance. The use of measured static flow resistive and corrected viscous length in the calculations are useful to cope with such a situation. Otherwise, the use of an optimized simple model as a function of flow resistivity is also applicable for this case.

Keywords: woven fabric; prediction model; sound absorber; building applications.

1. Introduction

Sound absorbers are principle parts of sound controls. For building applications, woven fabrics are usually applied as interior finishing of walls, ceiling, furniture and curtain (LARSEN, WEEKS, 1975). Apart from this, in some cases, the woven fabrics are employed as screen protector of mineral fibre absorbers like Rockwool and glass wools in order to prevent the mineral fibres being harmful to occupants. Hence, the woven fabrics are not designated as absorbers by design.

It is interesting to look at the property of fabrics, which have inherently microstructures, that is analogous to MPP structures. The basic construction of a MPP absorber consists of a thin flat panel that has sub-millimetre holes backed by a rigid wall with an air space between them. None of these components produce fibrous waste that harms health and environment. Consequently, the MPP absorbers are considered to be a basis for the next generations of sound absorbing system. Since pioneered by MAA (1975; 1987; 1998), many researches have been conducted to advance MPP absorbers technology for various purposes: rooms (FUCHS, ZHA, 2006; SAKAGAMI, MORIMOTO, 2008; SARWONO *et al.*, 2014), duct silencing (BRAVO *et al.*, 2014; WU, 1997), environmental noise (ASDRUBALI, PISPOLA, 2007), enhancing sound attenuation (HERRIN *et al.*, 2011; LIU, HERRIN, 2010), wideband absorbers (PRASETIYO *et al.*, 2016; QIAN *et al.*, ZHANG *et al.*, 2017), etc. However, mass production of these micro perforated panels with minute holes (of 0.1–0.3 mm) can be costly because of insufficient manufacturing technologies or specific technology requirements e.g. 3D printing (LIU *et al.*, 2017), MEMS technology (QIAN *et al.*, 2013).

Considering the microstructure of woven fabric, it is expected that the use of this material can deal with the harmful of fibrous porous absorbers as well as

the issue of cost in mass production of MPP. Moreover, the measurement results have confirmed the absorption capability of woven fabrics e.g. as reported in (DESENDRA *et al.*, 2017; SHOSHANI, ROSENHOUSE, 1990). Compared with other absorption systems, the MPP based woven fabric showing similar characteristic as found in other MPP and naturally differs from fibrous porous material particularly in terms of the absorption bandwidth (ARENAS, CROCKER, 2010; COX, D'ANTONIO, 2009).

From practical point of view, it is required to obtain absorber with proper sound absorption characteristics during design phase. Hence, a sound absorption model of woven fabrics is critical to be developed in order to predict their absorption coefficients. Moreover, such model is also important to make some advancements for a more complicated design or structure of the woven fabrics as sound absorber system. Recently, some efforts in modelling on fabric absorption have been conducted using porous membrane model under equivalent electrical circuit framework (PIEREN, 2012; PIEREN, HEUTSCHI, 2015). In this paper, the model will be derived using JCA framework (CHAMPOUX, ALLARD, 1991; JOHNSON *et al.*, 2006) in the context of multi-layer system. It differs from typical MPP absorber as discussed in (MAA, 1975); the pores of the woven fabric are formed by yarns and polymer that introduces perturbation to the perforation characteristics. Moreover, by choosing the JCA framework, it is expected that the resulting model can be easily incorporated to other absorber systems e.g. combining woven fabric and porous material to form a particular sound absorber system. Some analyses on the results are provided to discuss the model behaviour and its accuracy compared with the measured ones, particularly when the pore perturbations are present.

This paper is organized as follows: firstly, an introduction is presented to describe the motivation and the main objective of the paper. It is then followed by theoretical background; particularly JCA model and normal sound absorption model of woven fabric is derived subsequently. In Sec. 3, woven fabric properties are described and calculation results are presented for normal incidence sound wave case while experimental validations are conducted to evaluate the validity of model to the variation of woven fabric parameters. Moreover, some comparisons between the proposed model results and that of an optimized simple model as function of flow resistivity are provided. Lastly, some important results are summarized in conclusion.

2. Micro-perforated panel formulation

The micro-perforated panel can be formulated as a rigid frame based on Johnson-Champoux-Allard (JCA) model (CHAMPOUX, ALLARD, 1991; JOHNSON *et al.*, 2006). Five physical parameters are required in order to apply this model, that are open porosity ϕ, static flow resistivity σ, geometric tortuosity α_∞, viscous characteristic length Λ and thermal characteristic length Λ'.

Those five parameters are then used to define the dynamic mass density ρ_e and the dynamic bulk modulus K_e of woven fabric that can be deduced from JCA model as follows (CHAMPOUX, ALLARD, 1991; JOHNSON *et al.*, 2006)

$$\rho_e(\omega) = \rho_0 \alpha_\infty \left(1 + \frac{\sigma\phi}{j\omega\rho_0\alpha_\infty} G_j(\omega) \right), \qquad (1)$$

where

$$G_j(\omega) = \left(1 + j\frac{4\omega\rho_0\alpha_\infty^2\eta}{\sigma^2\phi^2\Lambda^2} \right)^{1/2}. \qquad (2)$$

The dynamic bulk modulus is expressed as

$$K_e(\omega) = \frac{\gamma P_0/\phi}{\gamma - (\gamma - 1)\,a^*}, \qquad (3)$$

where

$$a^* = 1 - j\frac{8\kappa}{\Lambda' C_p \rho_0 \omega}\sqrt{1 + j\frac{\Lambda'^2 C_p \rho_0 \omega}{16\kappa}}.$$

From the two formulations, the characteristic impedance Z_c and the complex wavenumber k_c of the woven fabrics can be obtained as follows

$$Z_c = \sqrt{\rho_e K_e}, \qquad (4)$$

$$k_c = \omega\sqrt{\frac{\rho_e}{K_e}}. \qquad (5)$$

The basic construction of woven fabric using MPP framework is presented in Fig. 1. It is basically consisting of a woven fabric backed up by air cavity and ended by an impervious layer. Using this construction
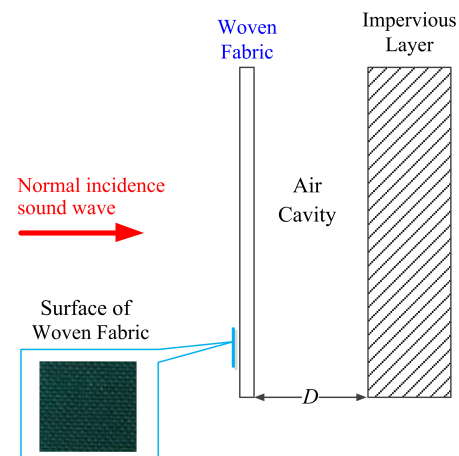

Fig. 1. Basic construction of woven fabric system considered in this study.

system, the normal surface impedance Z_s with a t thick woven fabric is

$$Z_s = Z_c \frac{-jZ_{ca}\cot(k_c t) + Z_c}{Z_{ca} - jZ_c\cot(k_c t)}, \qquad (6)$$

where $j = \sqrt{-1}$, $Z_{ca} = -j\phi Z_a\cot(kD)$ is the characteristic impedance of air in the cavity, ϕ is the open porosity or perforation rate of woven fabric, and D is the air cavity depth. Meanwhile, Z_a is the characteristic impedance of air.

Considering $kD \ll 1$ and $k_c t \ll 1$, Eq. (6) can be written as

$$Z_s \approx Z_c \frac{-jZ_{ca} + Z_c k_c t}{-jZ_c \left(1 - j\frac{\phi Z_a k_c t}{Z_c kD}\right)}. \qquad (7)$$

Furthermore, the fractional terms of bracket at the dominator is negligible compared to 1 under the following conditions:

1) $\phi < 1$ hold for the woven fabric cases so that the bulk modulus of woven K_e is comparable to that of the air in the cavity K_a.

2) The thickness of woven fabrics is much smaller than that of the air cavity depth ($t \ll D$).

Hence, Eq. (7) can be re-written as

$$Z_s = j\omega\rho_e t + Z_{ca}. \qquad (8)$$

The expression in Eq. (8) suggests that the formulation of woven fabric absorption essentially depends on the dynamic mass density of the woven fabric. In other words, the dissipative mechanism in the woven fabrics is dominated by the viscous-inertial effect rather than the thermal one. Moreover, all assumptions found in the JCA model are inherently present in the resulting model, i.e. rigid frame condition. The same result was also obtained by ATALLA and SGARD (2007) in modelling acoustic response of perforated screens.

By expanding Eq. (1), the effective density ρ_e can be re-written as follows

$$\rho_e = \rho_0\alpha_\infty - j\left[\left(\frac{\sigma\phi}{\omega}\right)^2 + j2\left(\frac{\rho_0\alpha_\infty\delta}{\Lambda}\right)^2\right]^{1/2}, \quad (9)$$

where $\sigma = 8\eta/\phi r_h^2$ with dynamic viscosity of air η and $\delta = \sqrt{2\eta/\rho_0\omega}$ is the viscous skin depth. The characteristic viscous length Λ for circular pore is typically equal to r_h. For the case of the woven fabrics, the following expression is preferable considering the varied cross section formed by the yarns, this is given by (ALLARD, 1993)

$$\Lambda = \frac{1}{c}\left(\frac{8\alpha_\infty\eta}{\sigma\phi}\right)^{1/2}, \qquad (10)$$

where c is the cross-sectional shape factors where its value is typically 1.07 for square pore (ALLARD, 1993).

Up to this point, the model incorporated in the calculations is denoted as standard model throughout this paper in which none of corrected or estimated parameters are introduced.

The high frequency expression of Eq. (9) gives

$$\lim_{\omega\to\infty}\rho_e = \alpha_\infty\rho_0\left(1 + \frac{\delta}{\Lambda}\right) - j\alpha_\infty\rho_0\frac{\delta}{\Lambda}. \qquad (11)$$

As $\omega \to 0$, the low frequency expression of ρ_e is

$$\lim_{\omega\to 0}\rho_e = \alpha_\infty\rho_0\left(1 + \frac{2\alpha_\infty\eta}{\sigma\Lambda^2\phi}\right) - j\frac{\sigma\phi}{\omega} \qquad (12)$$

which is equal to

$$\lim_{\omega\to 0}\rho_e = \alpha_\infty\rho_0\left(1 + \frac{\alpha_\infty}{4}\right) - j\frac{\sigma\phi}{\omega}, \qquad (13)$$

where $\sigma = 8\eta/\phi r_h^2$ and $\Lambda = r_h$ are considered. It is clear that the viscous characteristic length and the static flow resistivity controls the absorption behaviour at high and low frequency respectively.

Making use of real part of Eq. (11) and Eq. (12), the transition frequency of the flow resistivity control to the viscous characteristic length control is given by

$$f_{tr} = \frac{1}{4\pi\rho_0\eta}\left(\frac{\phi\Lambda\sigma}{\alpha_\infty}\right)^2. \qquad (14)$$

Lastly, considering a set of tubes exist on the same surface, the surface impedance becomes

$$Z_s' = j\frac{\omega\rho_e t}{\phi} - j\rho_0 c_0\cot(kD), \qquad (15)$$

where ρ_0 is the air density and c_0 is the speed of sound in air.

The normal sound absorption coefficient α_n is thus obtained as follows

$$\alpha_n = 1 - \left|\frac{Z_s' - \rho_0 c_0}{Z_s' + \rho_0 c_0}\right|^2. \qquad (16)$$

3. Model validation

3.1. Property of woven fabrics

To obtain geometry properties of the woven fabrics, the scanning electron microscope (SEM) was employed to capture the woven fabric images with magnification of about 30–40 times as shown in Fig. 2. The three kinds of woven fabric with different perforation properties are considered. The perforations of the woven fabrics are mostly square or nearly square. Polymer layers designated as fire-retardant are also present in some of them and become a perturbation to the pore properties. It should be noted that the parameters involved in calculations are characterized from commercial woven fabrics that are typically used for interior
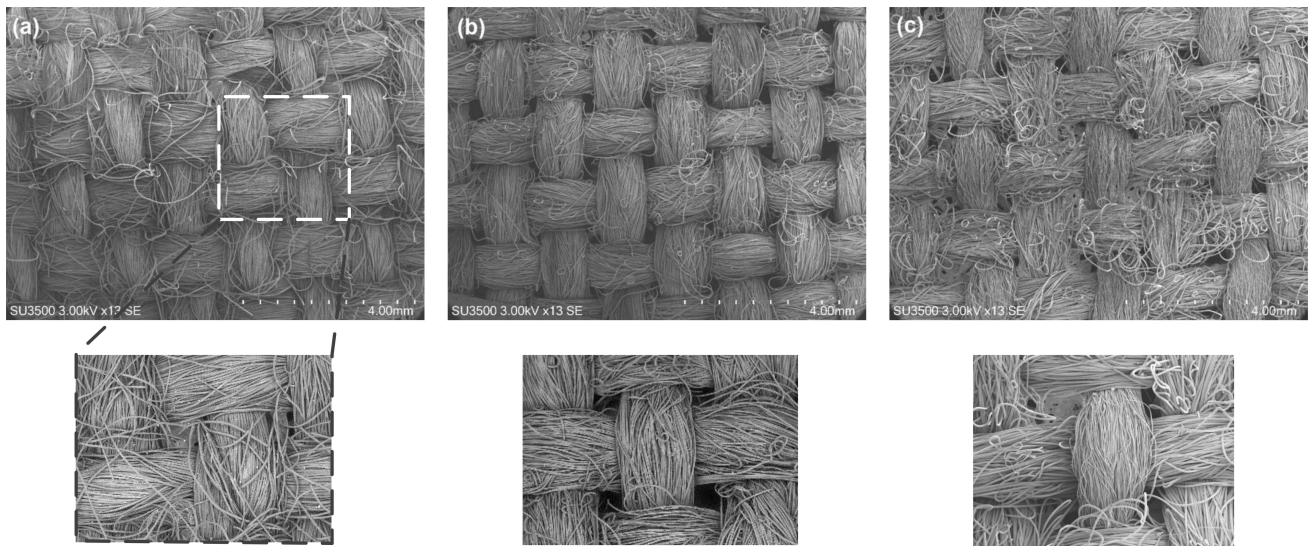
Fig. 2. Surface morphology of woven fabrics observed using SEM: a) Fabric 1; b) Fabric 2; c) Fabric 3. The dark area indicates through holes otherwise that consist of yarn or the polymer layer.

finishing. Perhaps, this is sufficient to test the model capabilities in predicting the sound absorption coefficients. Moreover, this is also expected that this study is more relevant to practical purposes aside from predicting model development itself.

The geometry properties of each woven fabric are listed in Table 1 after observing the surface morphology of each woven fabrics. For non-circular pores, the hydraulic radius of pore is defined as the ratio of pore area to its wetted perimeter which yields

$$r_h = 2\left(\frac{ab}{2(a+b)}\right) = \frac{ab}{(a+b)}, \qquad (17)$$

where a and b are the length of side. It should be noted that not all pores of the fabrics could be identified, i.e. in the case of the Fabric 1 where many pores situated between adjacent yarns are covered by a polymer layer, that acts as a flame-retardant layer, during manufacturing process. For this case, the acoustical parameters were obtained using approximation method as proposed by Jaouen (JAOUEN, BÉCOT, 2011). In the Fabric 3, several square pores are covered by a similar layer as found in the Fabric 1 but the rest of pore could still be identified using SEM measurements. All parameters obtained are then used as input for Eq. (15)

where a particular air cavity depth D is considered. Therefore, the normal sound absorption coefficients α can be calculated using Eq. (16).

3.2. Measurement method of sound absorption

For validation purposes, the absorption coefficient of woven fabrics were measured using impedance tube according to ISO 10534-2 (ISO, 1998). The schematic diagram of the measurement can be observed in Fig. 3. The speaker generated white noise and considered it as a plane wave travelling in tube with diameter of 3 cm and 10 cm for covering frequency of 64 to 6000 Hz. This plane wave conditions hold as the wavelength of the wave at the highest frequency was longer than the
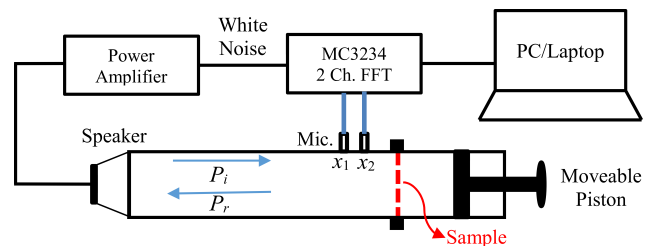

Fig. 3. Schematic diagram of sound absorption measurement using impedance tube.

Table 1. Average values for geometrical properties and estimated parameters of samples.

Sample	t [mm]	r_h [mm]	ϕ^*	σ [N·s/m⁴]	σ^* [N·s/m⁴]	$(\sigma \cdot t)$ [N·s/m³]
Fabric 1	0.90	0.106	0.035	–	$7.73 \cdot 10^5$	695.70
Fabric 2	0.50	0.154	–	$7.96 \cdot 10^4$	–	69.00
Fabric 3	0.50	0.206	–	$6.04 \cdot 10^4$	$1.30 \cdot 10^5$	30.20 (65.00)

* Estimated values obtained using the method in (JAOUEN, BÉCOT, 2011).

lateral tube diameter in order to avoid cross-section modes. By using transfer function of incoming wave pressure p_1 measured at microphone positions H_I as well as that of reflected wave pressures p_r measured at the same position H_R and combined with transfer function of total pressure at microphone 1 and 2, H_{12}, the reflection coefficient R can be defined as

$$R = \frac{H_{12} - H_1}{H_R - H_{12}} e^{jk_0 2x_1}. \tag{18}$$

Finally, the normal sound absorption coefficients of the woven fabric is obtained through

$$\alpha_n = 1 - |R|^2. \tag{19}$$

Each measurement lasted 120 seconds to ensure the steady state response of the system where 60 seconds for each microphone configuration is considered. Moreover, the absorption coefficients obtained from three time measurements were averaged.

An acrylic woven fabric holder was developed as a special mounting system, which did not alter the diameter inside the tube. The fabrics was held on the mounting as rigid as possible.

3.3. Results and discussion

Using geometry properties listed in Table 1 and the air properties in Table 2, calculations of normal sound absorption α_n for each fabric are performed. For the case of the Fabric 1, the estimated static flow resistivity and perforation rate are used in calculations due to the difficulty of identifying the actual through holes of the surface as presumably exist according to Eq. (9). The low frequency expression of ρ_e in Eq. (13) is employed to cover the sound absorption coefficients. Moreover, α_∞ is set to 1.

Table 2. Air properties are used in all studies.

c	ρ_0	η
343 m/s	1.21 kg/m^3	$1.81 \cdot 10^{-5}$ kg/(m·s)

The results can be observed from Fig. 4. As expected, the peak sound absorption frequency shifts toward lower frequency with increasing cavity depth following MPP absorber behaviour. It can also be seen that the prediction results tend to have greater deviations at high frequency ($f > 3500$ Hz) compared with that of the measurement ones. The deviation is reduced for greater cavity depth in which the absorption mostly exist at low and mid frequencies. This is further confirmed from the comparison result where 180 mm cavity depth is considered as is shown in Fig. 5. Obviously, the model can produce reasonable results except around the sound absorption peaks where the gap between the results enlarge as frequency increases.
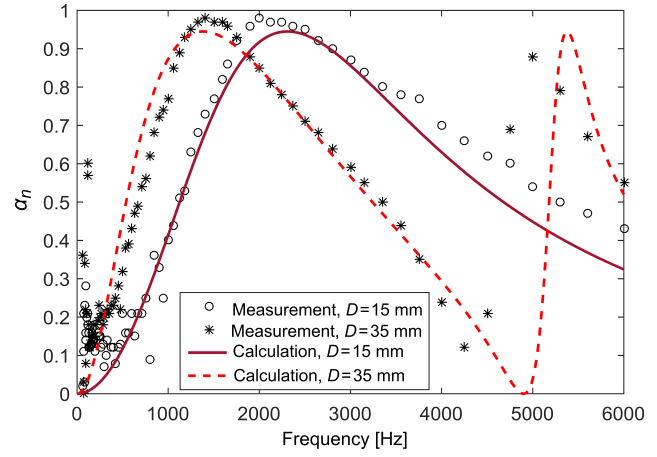

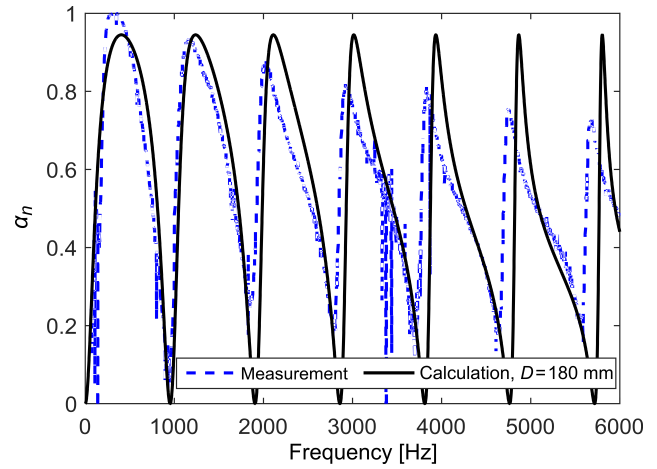Fig. 4. Sound absorption comparisons for the woven Fabric 1 with particular air cavity depths.

Fig. 5. Sound absorption comparisons for the woven Fabric 1 with a 180 mm cavity depth.

This comes about due to the higher structural acoustic modes interactions at resonance frequencies (LEE *et al.*, 2005) which is disregarded in the model.

Figure 6a and 6b present the sound absorption comparison of the Fabric 2 betwen calculation results and measurement ones for the case of 15 mm and 35 mm cavity depth respectively. All perforation parameters were obtained by SEM measurements. Hence, it is possible to use Eq. (9) for calculating the effective density of the woven fabrics rather than using the low frequency expression. Compared with the measurements results, it is clear that the model can produce reasonable results. The discrepancies between the results mostly observed at high frequency ($f > 3000$ Hz). The root mean square error (RMSE) of 0.09 is found for the case of 15 cavity depth.

As indicated by Eq. (11) to (13), the static flow resistivity σ and the characteristic viscous length Λ are responsible for the resistive terms in the effective density. Following the definition of σ there should be lesser issue with the terms as all pore parameters were ob-
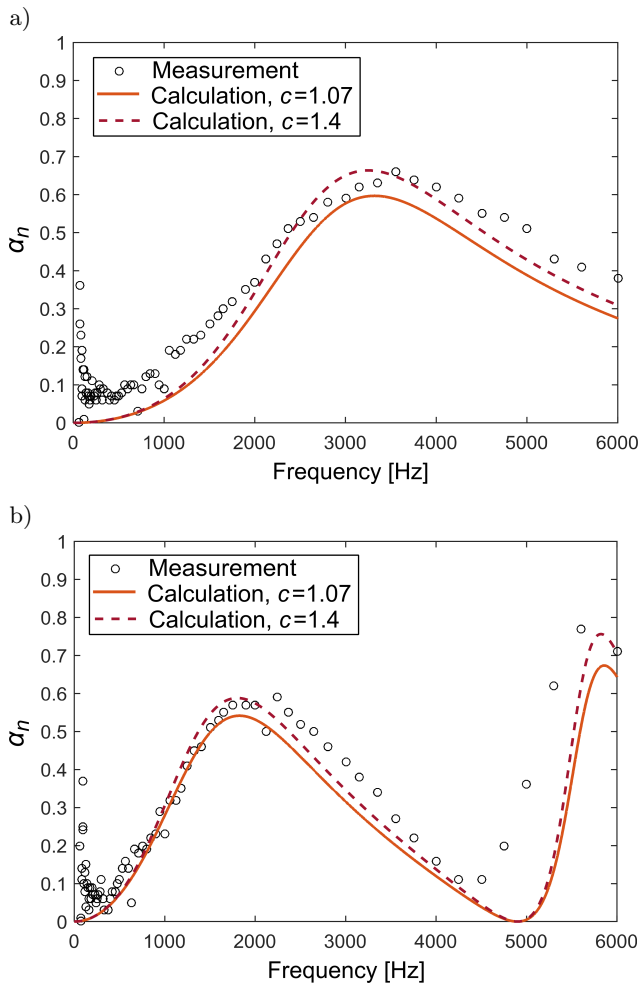
a)

b)

Fig. 6. Sound absorption comparisons for the woven Fabric 2 with particular cavity depths D: a) D = 15 mm, b) D = 35 mm.

tained by SEM as average values. It is expected that the value of σ is falling within the average value with the existing variance of the perforation. However, the SEM measurements could not directly capture the details of perforation in geometrical sense, i.e. the actual quantitative value of pore perimeter size and pore walls even though the pore shape can be observed visually. Moreover, the transition frequency f_{tr} of 2829 Hz is present indicating the discrepancy attributed to Λ control instead of σ.

To get better calculation results, a correction factor may be introduced to the characteristic viscous length Λ i.e. corrected shape factor c is set to 1.4. However, this approach lead to insignificant improvement where the RMSE of 0.07 for the case of 15 cavity depth. Hence, the results only differ by 0.02 point compared with that of standard model. Considering the errors, the standard model with typical c value of 1.07 as suggested by ALLARD (1993) is still applicable as long as the geometrical pore can be characterized.

It differs from the Fabric 1 and the Fabric 2, the Fabric 3 has its own surface morphology. As shown in

Fig. 2c, some of its perforation are not through holes due to the presence of thin polymer layer while other perforations are seen as square pores. The calculation approach are similar with that of the Fabric 2 where the standard model is employed. It is clear that the resulting absorptions are underestimated compared with that of the measurement as shown in Fig. 7a and 7b.
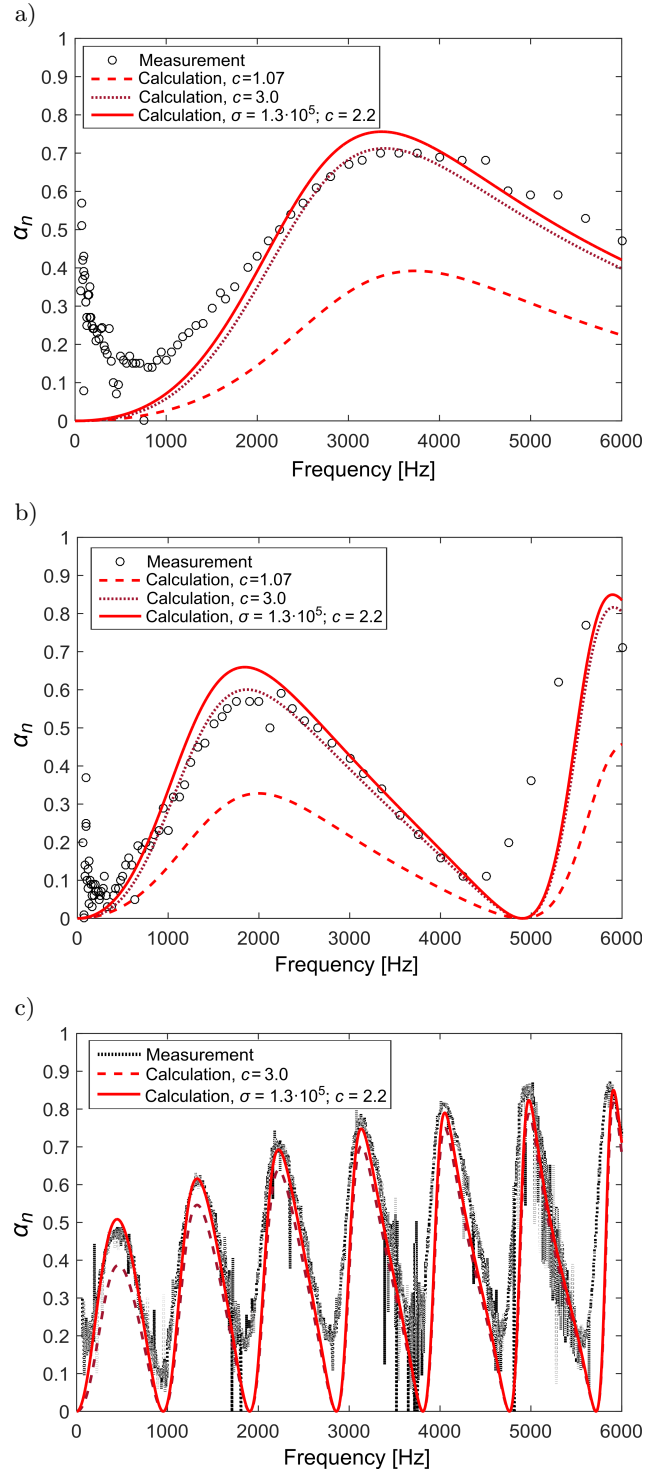
a)

b)

c)

Fig. 7. Sound absorption comparisons for the woven Fabric 3 with particular cavity depths D: a) D = 15 mm, b) D = 35 mm, c) D = 180 mm.

The sound absorption coefficient discrepancy between the calculation results and the measured one is up to 0.3 points.

Introducing corrected value of c make the results are closer to the measurement ones i.e. c is set to 3 by the same reason as the Fabric 2 case. However, considering the result for 180 mm cavity depth case, this approach is only successful at high frequency but not for low frequency where the absorption behaviours are still underestimated. By comparing the flow resistance obtained by calculation using Eq. (9) and measurements (see Table 1), it suggests that higher flow resistivity is required and more applicable for this case. To offset this condition, the use of corrected c value and the estimated flow resistivity altogether lead to better results for the case fabric with some of its pores covered by polymer layers such as the Fabric 3. For this, estimated flow resistivity of $1.3 \cdot 10^5$ N·s/m^4 and c value set to 2.2 leading the measurement and calculation are in agreement as shown in Fig. 7c. This approach can reduce the RMSE by 0.05 for low and mid frequency range ($f < 2500$ Hz).

3.4. Comparisons to simple flow resistivity model

A simple model as a function of flow resistivity parameter is employed to benchmark the predicting model results. For this, a basic model of Delaney-Bazley is considered where the characteristic impedance and complex wave number can be defined as follows (DELANY, BAZLEY, 1970)

$$z_c = \rho_0 c \left[1 + c_1 \left(\frac{\rho_0 f}{\sigma} \right)^{-c_2} - j c_3 \left(\frac{\rho_0 f}{\sigma} \right)^{-c_4} \right], \quad (20)$$

$$k_c = \frac{\omega}{c} \left[c_5 \left(\frac{\rho_0 f}{\sigma} \right)^{-c_6} - j c_7 \left(\frac{\rho_0 f}{\sigma} \right)^{-c_8} \right], \quad (21)$$

where c_i ($i = 1 \ldots 8$) is the numerical constants. The total of surface impedance is then calculated using Eq. (6) by making use of z_c and k_c in Eqs. (20) and (21) and also combining with Z_{ca}. The values of c_i are obtained through optimization approach by adopting the Nelder-Mead simplex method and applied following the procedure in (ARENAS *et al.*, 2014) to minimize a cost function of squared difference between the measured absorption coefficients and corresponding predicted absorption coefficients. Hence, essentially the simple model considered here is an empirical model.

For the comparison purposes, the simple model is only run for frequency 500 Hz up to 6 kHz. Meanwhile, the flow resistivity data are obtained from Table 1 while the case of 15 mm air cavity is considered. The optimization approach yields the numerical constants c_i and listed in Table 3. It should be noted that the highest value of absorption coefficient around sound absorption peak is included in the optimization process in order to get better c_i values.

Figure 8 presents the comparison results between the absorption coefficients calculated by the JCA model and that of the simple model. The results are then compared with the measured absorption coefficients. It is clear that the simple model optimized using empirical data can produce absorption coefficients in a good agreement with the measured ones particularly for the cases of inconclusive pore geometry woven fabrics i.e. Fabric 1 (see Fig. 8a) and Fabric 3 (see Fig. 8c). A different result is observed for the case of the Fabric 2 as shown in Fig. 8b where the simple model results have discrepancies with the measured ones particularly around the peak of sound absorption and high frequency while the JCA model based can predict the absorption coefficient reasonably using the perforation parameter without introducing correction factors or optimized values. To be fair, the use of simple model can be useful when the parameter model cannot be concluded due to the complexity in pore geometry as long as empirical sound absorption coefficient data is available for obtaining optimized correction factors. Other than that, the use of parametric model like the JCA is more beneficial in terms of optimization purposes in order to develop the woven fabric absorption further to meet particular absorption characteristics.

4. Conclusions

A sound absorption prediction of woven fabric has been performed using a model derived based on JCA formulation framework. For the case of the woven fabric with inconclusive pore geometry, the use of approximate static flow resistive is useful in which the sound absorption coefficient can be covered using low frequency expression. More complex conditions are present for the case of woven fabric with polymer layers in some of pores. For this case, the pore geometry obtained cannot represent the actual resistivity of the woven fabric. Hence, predicted sound absorption coeffi-

Table 3. Numerical constants c_i obtained using the Nelder-Mead simplex method.

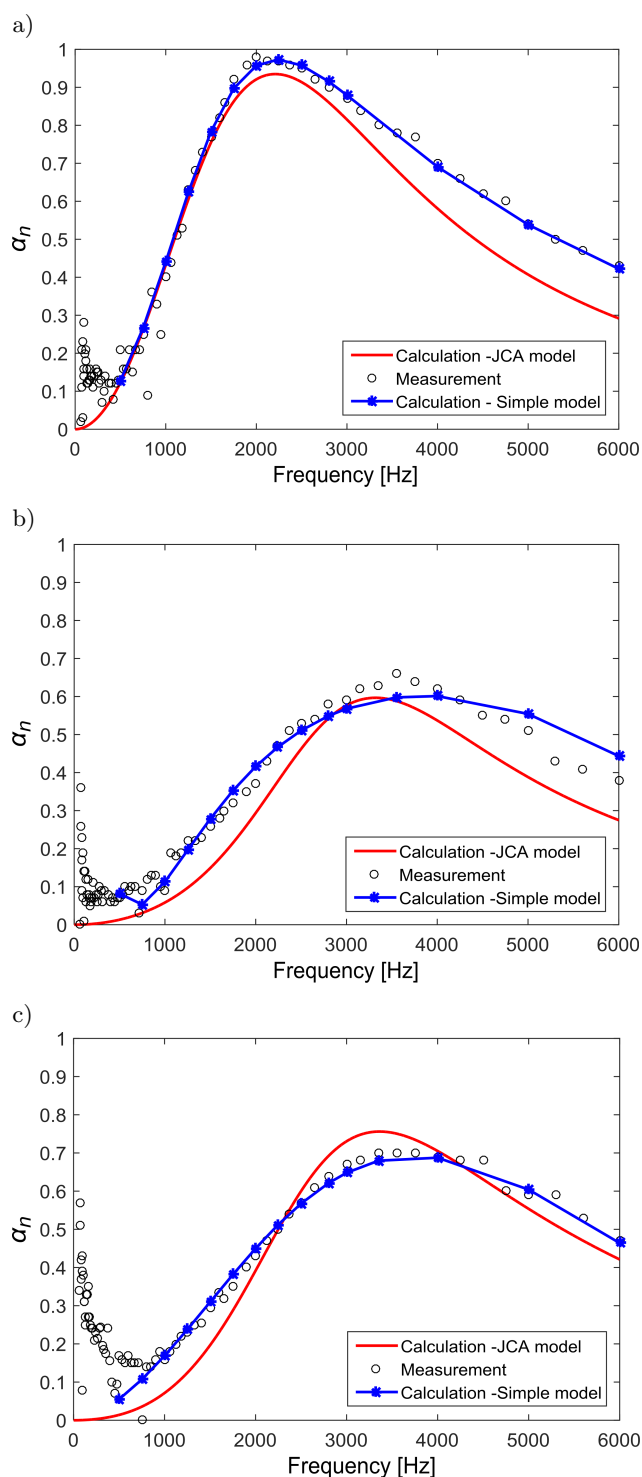| Sample	Numerical constant							
	c_1	c_2	c_3	c_4	c_5	c_6	c_7	c_8
Fabric 1	0.1005	1.4115	0.4140	−4.7685	1.8606	−0.4763	0.0685	−0.0059
Fabric 2	0.0023	1.3825	0.1330	0.5966	0.2167	1.3635	−0.0324	0.2983
Fabric 3	0.3358	2.4900	0.0450	3.1774	2.8969	−1.8534	−5.6723	−2.4259

a)

b)

c)

Fig. 8. Sound absorption comparison between JCA model and simple model calculations to the measurement ones for the case of 15 mm air cavity depths: a) Fabric 1, b) Fabric 2, c) Fabric 3.

simple model like the Delany-Bazley model is also applicable for such cases as long as empirical data is available. None of estimated parameters or corrected viscous length is required for woven fabric with fully characterized perforation where the standard calculation procedure for the JCA model based can produce reasonable results. The results indicate that the standard model is only applicable for the woven fabrics with perforations characteristic fully identified otherwise the resistive component of surface impedance is inaccurate as a result of pore perturbation implications.

Acknowledgment

References

1. ALLARD J.F. (1993), *Propagation of Sound in Porous Media*, Elsevier, London.

2. ARENAS J.P., CROCKER M.J. (2010), *Recent trends in porous sound-absorbing materials*, Sound and Vibrations, **44**, 12–17.

3. ARENAS J.P., REBOLLEDO J., DEL REY R., ALBA J. (2014), *Sound absorption properties of unbleached cellulose loose-fill insulation material*, BioResources, **9**, 4, 6227–6240.

4. ASDRUBALI F., PISPOLA G. (2007), *Properties of transparent sound-absorbing panels for use in noise barriers*, Journal of the Acoustical Society of America, **121**, 1, 214–221.

5. ATALLA N., SGARD F. (2007), *Modeling of perforated plates and screens using rigid frame porous models*, Journal of Sound and Vibration, **303**, 1, 195–208, https://doi.org/10.1016/j.jsv.2007.01.012.

6. BRAVO T., MAURY C., PINHÉDE C. (2014), *Microperforated panels for silencers in ducted systems*, paper presented at the Forum Acusticum, Kraków, 2014-09-07, Poland.

7. CHAMPOUX Y., ALLARD J.F. (1991), *Dynamic tortuosity and bulk modulus in air-saturated porous media*, Journal of Applied Physics, **70**, 4, 1975–1979, doi: 10.1063/1.349482.

8. COX T.J., D'ANTONIO P. (2009), *Acoustic Absorbers and Diffusers*, Taylor and Francis, London.

9. DELANY M.E., BAZLEY E.N. (1970), *Acoustical properties of fibrous absorbent materials*, Applied Acoustics, **3**, 2, 105–116, https://doi.org/10.1016/0003-682X(70)90031-9.

10. DESENDRA G., HERMANTO M.N., PRASETIYO I., ADHIKA D.R. (2017), *Experimental investigation of fabric-based micro perforated panel absorber*, paper presented at the RECAV, Bali.

cients of the standard model are underestimated while introducing corrected viscous length only improves the result of mid and high frequency. The combination of estimated flow resistivity and corrected viscous length is useful in this case. Moreover, the use of optimized

11. FUCHS H.V., ZHA X. (2006), *Micro-perforated structures as sound absorbers – a review and outlook*, Acta Acustica united with Acustica, **92**, 1, 139–146.

12. HERRIN D.W., LIU J.H., SEYBERT A. (2011), Properties and applications of microperforated panels, Sound & Vibration, **45**, 6–9.

13. ISO (1998), *Standard 10534-2 Acoustics – Determination of sound absorption coefficient and impedance in impedance tubes – Transfer function method.*

14. JAOUEN L., BÉCOT F.X. (2011), *Acoustical characterization of perforated facings*, The Journal of the Acoustical Society of America, **129**, 3, 1400–1406, doi: 10.1121/1.3552887.

15. JOHNSON D.L., KOPLIK J., DASHEN R. (2006), Theory of dynamic permeability and tortuosity in fluid-saturated porous media, Journal of Fluid Mechanics, **176**, 379–402, doi: 10.1017/S0022112087000727.

16. LARSEN J.L., WEEKS J.G. (1975), *Fabrics for interiors: a guide for architects, designers, and consumers*, Wiley.

17. LEE Y.Y., LEE E.W.M., NG C.F. (2005), *Sound absorption of a finite flexible micro-perforated panel backed by an air cavity*, Journal of Sound and Vibration, **287**, 1, 227–243, https://doi.org/10.1016/j.jsv.2004.11.024.

18. LIU J., HERRIN D.W. (2010), *Enhancing micro-perforated panel attenuation by partitioning the adjoining cavity*, Applied Acoustics, **71**, 2, 120–127, https://doi.org/10.1016/j.apacoust.2009.07.016.

19. LIU Z., ZHAN J., FARD M., DAVY J.L. (2017), *Acoustic properties of multilayer sound absorbers with a 3D printed micro-perforated panel*, Applied Acoustics, **121**, 25–32, https://doi.org/10.1016/j.apacoust.2017.01.032.

20. MAA D.-Y. (1975), *Theory and design of microperforated panel sound-absorbing constructions*, Scientia Sinica, **18**, 1, 55–71, https://doi.org/10.1360/ya1975-18-1-55.

21. MAA D.-Y. (1987), *Microperforated-panel wideband absorbers*, Noise Control Engineering Journal, **29**, 3, 77–84, doi: 10.3397/1.2827694.

22. MAA D.-Y. (1998), *Potential of microperforated panel absorber*, The Journal of the Acoustical Society of America, **104**, 5, 2861–2866, doi: 10.1121/1.423870.

23. PIEREN R. (2012), *Sound absorption modeling of thin woven fabrics backed by an air cavity*, Textile Research Journal, **82**, 9, 864–874, doi: 10.1177/0040517511429604.

24. PIEREN R., HEUTSCHI K. (2015), *Predicting sound absorption coefficients of lightweight multilayer curtains using the equivalent circuit method*, Applied Acoustics, **92**, 27–41.

25. PRASETIYO I., SARWONO J., SIHAR I. (2016), *Study on inhomogeneous perforation thick micro-perforated panel sound absorbers*, Journal of Mechanical Engineering and Sciences (JMES), **10**, 3, 2350–2362.

26. QIAN Y.J., KONG D.Y., LIU S.M., SUN S.M., ZHAO Z. (2013), *Investigation on micro-perforated panel absorber with ultra-micro perforations*, Applied Acoustics, **74**, 7, 931–935, https://doi.org/10.1016/j.apacoust.2013.01.009.

27. QIAN Y.J., ZHANG J., SUN N., KONG D.Y., ZHANG X.X. (2017), *Pilot study on wideband sound absorber obtained by adopting a serial-parallel coupling manner*, Applied Acoustics, **124**, 48–51, https://doi.org/10.1016/j.apacoust.2017.03.021.

28. SAKAGAMI K, MORIMOTO M. (2008), *Application of microperforated panel absorbers to room interior surfaces*, International Journal of Acoustics and Vibration, **13**, 3, 120–124.

29. SARWONO J., PRASETIYO, I., ANDREAS S., WILLIAM A. (2014), *The design of MPP and its application to enhance the acoustics of a real auditorium*, paper presented at the Inter-Noise 43rd International Congress on Noise Control Engineering, Melbourne.

30. SHOSHANI Y., ROSENHOUSE G. (1990), *Noise absorption by woven fabrics*, Applied Acoustics, **30**, 4, 321–333, https://doi.org/10.1016/0003-682X(90)90081-5.

31. WU M.Q. (1997), *Micro-perforated panels for duct silencing*, Noise Control Engineering Journal, **45**, 69–77.